Available online at www.sciencedirect.com

ScienceDirect

Energy Procedia 00 (2015) 000–000

Energy Procedia

www.elsevier.com/locate/procedia

5th Workshop on Metallization of Crystalline Silicon Solar Cells

Dispensing Technology on the Route to an Industrial Metallization Process

Maximilian Pospischil[a]*, Martin Kuchler[a], Markus Klawitter[a], Carlos Rodríguez[a], Milan Padilla[a], Raphael Efinger[a], Michael Linse[a], Angel Padilla[a], Harald Gentischer[a], Markus König[b], Matthias Hörteis[b], Lars Wende[c], Oliver Doll[d], Roland Zengerle[e], Florian Clement[a] and Daniel Biro[a]

[a]*Fraunhofer Institute for Solar Energy Systems (ISE), Heidenhofstr. 2, D-79110 Freiburg, Germany*
[b]*Heraeus Precious Metals GmbH & Co. KG, Electronic Materials Division, Business Unit Photovoltaics, Heraeusstr. 12-14, D-63450 Hanau, Germany*
[c]*ASYS Automatisierungssysteme GmbH, Solar & New Technologies, Benzstr. 10, D-89160 Dornstadt, Germany*
[d]*Merck KGaA, Performance Materials Division, Postcode Q004/001, Frankfurter Str. 250, D-64293 Darmstadt, Germany*
[e]*Department of Microsystems Engineering – IMTEK, University of Freiburg, Georges-Köhler-Allee 103, D-79110 Freiburg, Germany*

Abstract

This study presents a new developed, inline applicable dispensing platform that is equipped with an advanced version of previously introduced parallel dispensing print heads and works as drop-in-replacement in existing manufacturing lines. At process speeds of up to 700 mm•s-1 and a substantially improved process stability, the impact of the resulting contact geometries on optical and ohmic losses was analysed in detail. A reduced finger width as well as an effective width of just 48% after encapsulation of the finger width leads to nearly 50% reduction of shading losses compared to screen printed samples. A substantially improved finger homogeneity leads to similar grid resistances at 20% less silver consumption.
Consequently, recent cell results on industrial emitters (R_{sh} = 90 Ω/sq.) showed an efficiency increase of up to +0.4%abs. in comparison to standard single screen printing technology. Top values of η = 19.4% using standard Al-BSF technology and η = 20.5% using PERC technology were reached in this study. A key improvement of the technology is the new ability to process certain metal pastes originally designed for screen printing applications and thus keep in track with fast emerging paste development. Successfully evaluated screen printing pastes then can be rheologically adapted in order to reach ultrafine contact fingers at high aspect ratios and extract the whole advantage of this non-contacting printing technology.

© 2014 The Authors. Published by Elsevier Ltd.
Peer-review under responsibility of the scientific committee of the SiliconPV 2014 conference.

* Corresponding author. Tel.: +49 761 4588 5268
E-mail address: maximilian.pospischil@ise.fraunhofer.de

1876-6102 © 2015 The Authors. Published by Elsevier Ltd.
Peer-review under responsibility of Gunnar Schubert, Guy Beaucarne and Jaap Hoornstra.

Keywords: silicon, solar cells, printing, metallization, dispensing, contact geometries, economic evaluation, analytic simulation

1. Introduction

Silicon solar cell metallization is still dominated by screen printing technology offering a robust contact formation and proven long term stability. Forced by a rapid decline of retail module prices, Ag-paste consumption had to be substantially reduced [1]. Consequently, paste and process development were pushed to achieve printed line widths of less than 50µm. However, known issues like mesh marks, line spreading or screen wear have not yet overcome. Different thick film technologies like stencil printing [2] or recently introduced co-extrusion approach [3] are promising technologies but are challenged by high consumable costs in the former or the competition of fast emerging screen printing pastes that cannot be directly used in the latter approach.

The dispensing technology, as described by Specht et al. [4], offers a contactless, high-throughput single-step metallization process significantly reducing finger width and thus shading losses. Record cell efficiencies of *20.6%* on *125x125mm² FZ p-type* material using dispensing technology on MWT-PERC (Metal Wrap Through – Passivated Emitter and Rear Cell) solar cells, featuring a selective emitter structure were presented by Lohmüller et al. [5]. Dispensing pastes are directly derived from screen printing paste development [6] and resulting finger geometries can be varied in a wide range by adapting paste rheology as described in previous studies e.g. [7]. In order to demonstrate the benefit of these advantages, the analytical 2D simulative tool Gridmaster [8] was enhanced to observe the effect of various geometrical parameters on solar cell results and manufacturing costs [9]. Both however, imply a stable metallization process at high throughput rates. For this reason, a novel dispensing platform was developed, providing fully automated inline production feasibility. In the following, this platform, was equipped with an advanced parallel dispensing print head as introduced in [10] and applied for extensive solar cell processing. Here, a focus was put on process stability using latest industrially manufactured dispensing pastes with sufficient contacting behavior on state of the art emitters (R_{sh} > 90 Ω/sq.).

Nomenclature

A_f (µm²)	finger cross-section area	R_{sh} (Ω/sq.)	Emitter sheet resistance
D (µm)	nozzle outlet diameter	V_{oc} (mV)	open circuit voltage
EW (%)	effective finger width	w_{BB} (µm)	busbar width
FF (%)	fill factor	w_c(µm)	contact width
j_{sc} (mA/cm²)	short circuit current	w_s(µm)	screen opening width for single and double screen printed reference samples
N (-)	Number of contact fingers	w_o (µm)	optical (= max.) finger width
r_{Bulk} (Ω·cm)	bulk resistivity		
r_f (µ Ω·cm)	finger resistivity	ρ_c (mΩ·cm²)	contact resistivity
R_{Grid} (Ω/m)	finger grid resistivity	η (%)	solar cell conversion efficiency

2. Approach

The focus of three years lasting research project “GECKO” was mainly the development of dispensing technology aiming on an industrial implementation. Here, precise rheological analysis of dispensing pastes [7, 10] and a subsequent implementation of a rheological paste model allowed for an efficient development of parallel print heads by computational fluid dynamic (CFD) simulations [10, 11].

After providing a homogeneous mass flow distribution to all nozzles and optimizing the shape of the incorporated nozzle plates, record finger widths of just 27µm were demonstrated using previous paste generations [10]. During this study, development was focused on providing high process stability with new developed silver pastes at competitive finger geometries. For this reason a novel, fully automated dispensing platform incorporating

the parallel dispensing unit [6] was launched and applied for processing of different solar cell batches on industrial preprocessed 156 x 156 mm² Cz p-type Silicon material of both, standard Al-BSF and PERC technology.

Resulting finger geometries were analyzed in detail regarding their influence on optical and ohmic losses. Here, results obtained from laser electron microscopy (LEXT) as well as LBIC measurements were combined to determine all relevant geometrical parameters for optical losses. Here an approach introduced by Beutel et al. [3] was applied to determine the effective width of different pastes and printing technologies on cell level and after module encapsulation. Ohmic losses depending on finger geometry are mainly related to the finger cross section. Here, values of finger grid resistivity R_{Grid} were correlated with wet paste consumption giving an indication of the effective silver usage of the different applied technologies.

3. Results and discussion

3.1. Improving printing pastes

Due to the non-contact printing process, dispensing offers the possibility to adapt paste rheology in a much wider range than other thick film printing technologies. For this reason, the shape of resulting contact fingers on the wafer can be adjusted with respect to an optimum trade-off between mechanical robustness, shading losses and electrical contacting behaviour.

However, recent paste development in screen printing technology addresses fine line printing in order to save material costs. The characteristics of these pastes resemble more and more those required for dispensing pastes. This brings a huge advantage, since new results and findings from screen printing paste development can be directly transferred to dispensing technology. In a first step, new paste systems are then evaluated regarding their applicability for dispensing. Here, very homogeneous finger geometries (Fig. 1) were obtained but with medium aspect ratio. Once, the evaluation of a novel paste has been successful, paste rheology has to be adapted towards higher yield stresses allowing for even more beneficial finger geometries with high aspect ratios and substantially reduced line widths (Fig. 2).

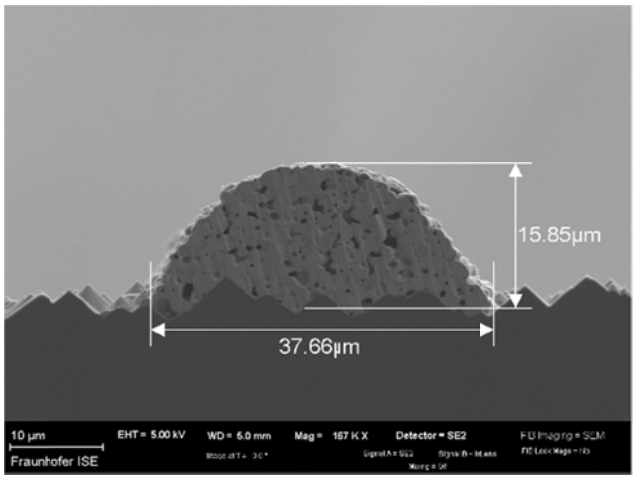

Fig. 1 Finger cross section of dispensed contact fingers using a new developed screen printing paste, printed in a parallel dispensing unit with a nozzle opening of just 40µm.

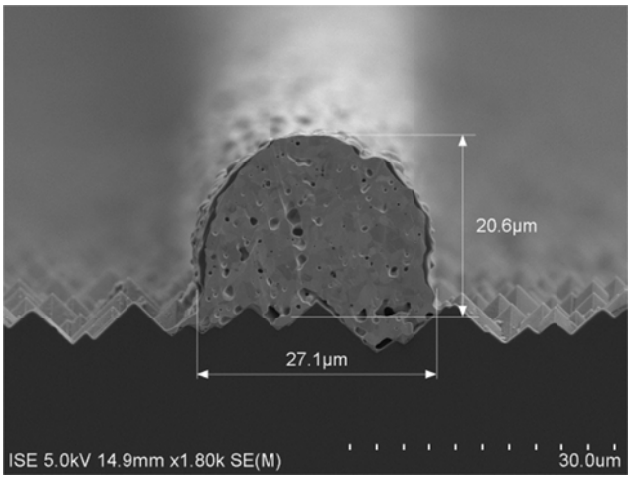

Fig. 2 SEM picture of finger cross section of dispensed contact fingers using a dispensing paste with adapted rheology [10], printed in a parallel dispensing unit with a nozzle opening of just 40µm.

3.2. Development of multi nozzle print heads

In order to significantly increase throughput rates during dispensing, a novel parallel print head was developed. For this reason, rheological paste characteristics were used to implement an universal paste model including Non-Newtonian flow patterns like shear thinning and yield stress [10]. After verifying this paste model using a single nozzle dispense setup, the focus was put on the development of a ten nozzle parallel dispensing prototype (Fig. 3). Here, a modular setup allowed for a separate optimization of dispensing nozzles, valves and paste distribution.

In the following, multi nozzle print head designs were tested and optimized regarding their robustness concerning fabrication tolerances. Due to specially designed nozzles, the necessary dispensing pressure was reduced by a factor of up to ten compared to commercial standard nozzles. A central fed paste supply with nozzle pitches of only 1.56 mm was realized which allows for further scalability of the design in the future.

3.3. Integration into an inline applicable platform

Finally, the novel print head was integrated in a newly developed fully automated dispensing platform (Fig. 4) which permits industrial manufacturing sequences with the new setup. Here, a fully automated cell handling system allows for a precise application of dispensed grid structures on industrial solar cells.

Continuous line dispensing at line speeds of more than 700 $mm \bullet s^{-1}$ was already reached using this setup. Furthermore, a nozzle distance of just 50 µm can be realized during dispensing with this platform. However, rheological adaptions of the dispensing pastes also allow for a stable process at much greater distances by stretching the paste during its free flow phase.

3.4. Concepts for Inline Integration

Most standard back-end production line concepts consist of three subsequent printing steps. Two are needed for the back surfaces, namely printing of Aluminum providing a full area contact of the p-type base and local silver pads that are required for soldered module interconnection. The front side grid is finally printed using a third screen printer which is followed by the fast firing oven (FFO) as visible in Fig. 5, top route. In order to further increase cell efficiencies, various routes with four printers in series have been introduced, mainly dual and double printing. The former allows for a reduction of recombination losses and silver consumption by applying a specially designed, non-contacting busbar paste (i.e. floating busbar concept [12]). Here, contact fingers are alternatively applied by stencil printing. The latter (i.e. double printing or print on print) increases finger aspect ratio (AR) and reduces the influence of mesh marks by adding a second printing step that is precisely aligned to the first one, see Fig. 5, second route.

The integration of the inline dispensing platform states the third route in Fig. 5. Here, a conventional busbar printing step is followed by the application of the dispensed finger grid before entering the FFO. In opposite to all previous routes, the contact less dispensing step does not require a previous drying step which allows for a further reduction of investment costs and foot print of the tool. With all other back end steps remaining the same, the integration of a dispensing unit can be seen as drop-in-replacement compared to all other dual or double printing approaches. With line speeds of more than 700 $mm \bullet s^{-1}$, the expected through put of the back-end production line by far is not limited by the dispensing process. Moreover, even a junction of two parallel printing lines into one dispensing unit is possible providing that the print head contains a sufficient number of parallel operating dispensing nozzles.

Fig. 3 Advanced version of the ten nozzle print head during cell manufacturing within the new dispensing platform.

Fig. 4 Completely new developed, inline applicable dispensing platform at Fraunhofer ISE's PV-TEC.

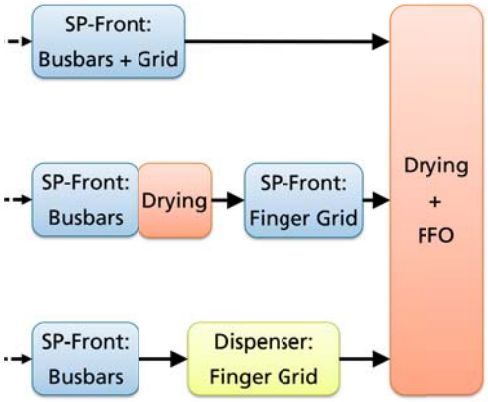

Fig. 5 Concepts for inline integration of different printing approaches. Standard single printing (top route) is compared with dual/double printing (second route) and dispensing (bottom route).

3.5. Influence of contact finger geometry on cell results

Once, a stable dispensing process at high through put rates has been established and applied metal pastes show similar electrical behavior the expected cell and module results highly depend on the geometrical shape of the contact finger. The optical finger width w_o is directly linked to the corresponding metal coverage of the cell and thus influences both, shading as well as recombination losses underneath the contacts. For the three setups applied in this comparison, it decreases from $w_o = 53\mu m$ for the single screen printed reference to around $35\mu m$ for the dispensing process when applying a nozzle plate with opening diameter of $D = 40\mu m$.

On the other hand, the resulting finger cross section A_f has a strong influence on grid resistance R_{Grid} as well as silver consumption, since a constant number of contact fingers was applied to all technologies ($N = 100$). Here, corresponding values of the dispensing processes with nozzle plates of $D = 50\mu m$ and $D = 40\mu m$, respectively were slightly lower than those obtained for both reference technologies (screen printing and double screen printing).

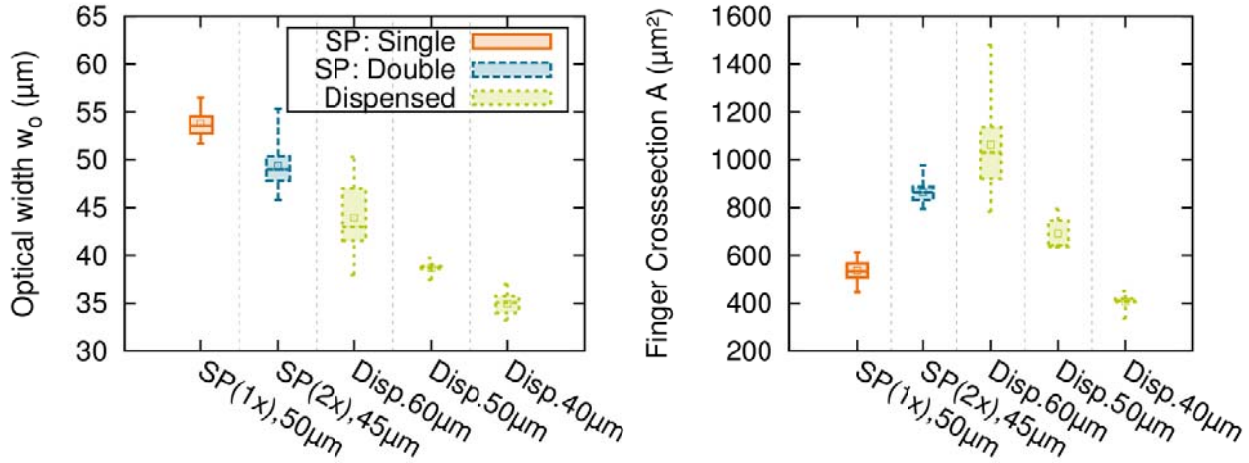

Fig. 6 Optical finger width (left) wo and corresponding finger cross section (right) of different printing technologies with indicated screen opening width w_s and nozzle opening diameter D, respectively.

However, another advantage of the dispensing process is its substantially increased finger homogeneity (Fig. 7) that allows to print extremely fine lines without drawbacks coming from mesh marks or paste spreading that both lead to additional silver consumption that does not contribute to lateral current transport within the fingers. In order to illustrate this effect, wet paste consumption of various printing experiments on industrial Cz material with both technologies was plotted against the values of the grid resistance R_{Grid} (Fig. 8) obtained from IV-measurement of the corresponding solar cells.

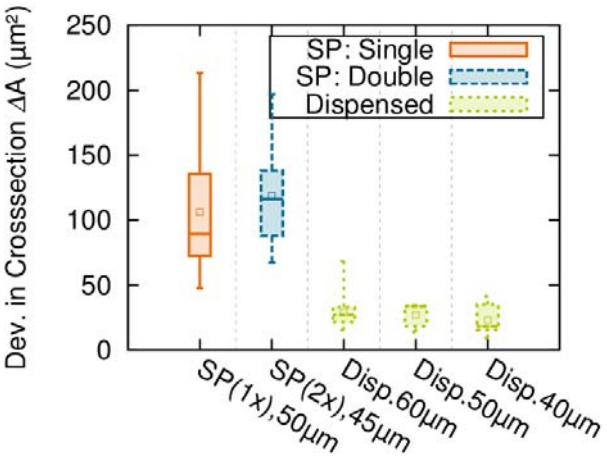

Fig. 7 Comprison of finger homogeneity of the applied technologies by means of the standard deviation in finger cross section area A_f.

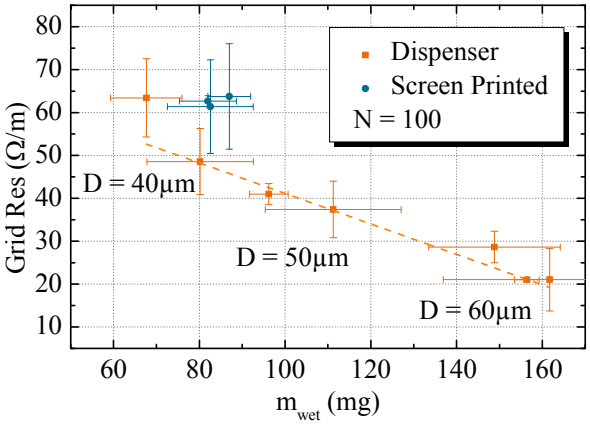

Fig. 8 Correlation of wet paste consumption and grid resistance R_{Grid} for dispensing and screen printed solar cells, respectively.

As expected, a linear correlation between paste consumption and R_{Grid} is clearly visible for all dispensed contact fingers with a homogeneous finger cross section A_f. All screen printed solar cells however suffer from an increased grid resistance at similar paste consumption that implies that the effective silver usage is reduced by around 20% compared to dispensed finger grids.

3.6. Influence of finger shape: Determination of effective finger width

To assess the desired optical coupling of light bouncing from a finger back onto the cell surface, we evaluated the relative effective widths (EW) for all compared metallization technologies on a cell and module level. We defined the effective as in [13] as the fraction of effective shading and theoretical geometrical shading defined by the finger width. Our EW determination method of choice was using spectrally resolved light-beam induced current measurements (SR-LBIC). The measurement and evaluation is similar to the one recently proposed by Beutel et al. [3]. In this work however, the reflectance of surface texture was not regarded as part of the solar cell shading. Furthermore, EW was determined for six wavelengths from 405 nm to 1064 nm to account for spectral dependence over the relevant range. The resulting spectrally dependent EW curve was weighed with the AM 1.5G spectrum as well as the solar cells external quantum efficiency (EQE) for an EW value representative to standard testing conditions. More details on this approach and the uncertainties of other EW determination methods will be discussed elsewhere.

The results of the applied printing technologies can be seen in Fig. 9. Here, single and double screen printing was compared with a sample with dispensed screen printing paste and one with a rheologically optimized dispensing paste with high aspect ratios (AR).

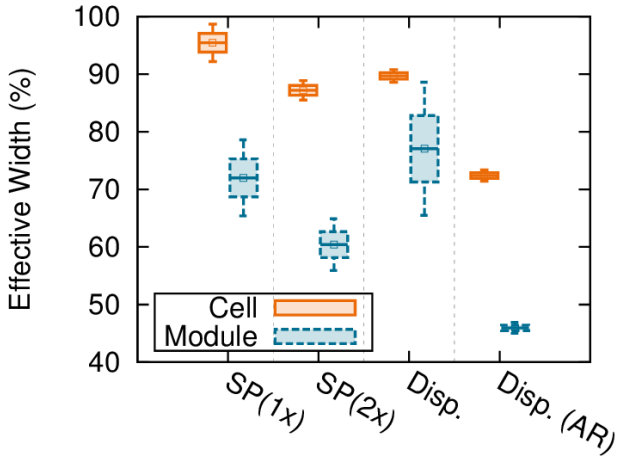

Fig. 9 Effective finger widths on cell and module level in comparison for different printing technologies.

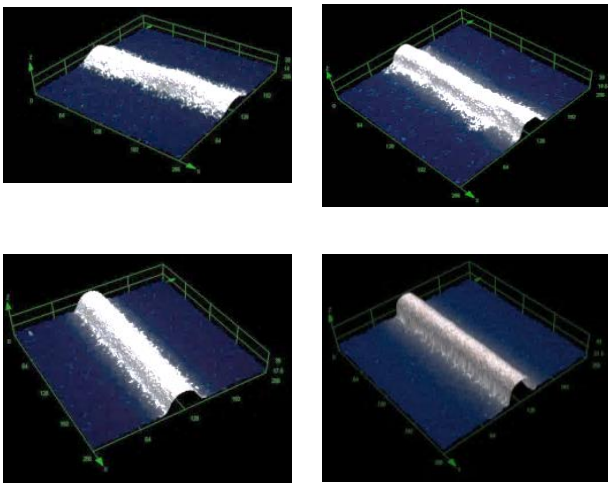

Fig. 10 Comparison of finger cross sections of the four applied technologies. Single and double screen printing are depicted in the top row, the two dispensed fingers with ordinary paste and rheologically adapted paste in the bottom row.

The effective widths on cell and module level decrease from single screen printed to double printed and dispensed samples with high aspect ratio. The value of the sample with dispensed screen printing paste however remains in the range of the screen printed samples, probably due to a severe impact of paste spreading. As a consequence, paste evaluation regarding printability and electrical behavior can easily be performed with pastes designed for screen printing. For cell and module production however, a rheological paste adaption leads to a substantial reduction of EW and certainly should be taken into consideration. However, note that the EW value on the module level also depends on the specific encapsulation materials, choice of front glass, glass coating etc. which will be subject to future studies in the field.

3.7. Solar cell results on Al-BSF (optional)

Early studies showed that an efficiency increase of around 2-3% rel. compared to screen printed solar cells is reached by replacing standard screen printed front contacts by high aspect ratio, ultrafine dispensed contact fingers . In order to make use of this benefit, especially the electrical performance of applied dispensing pastes has to keep up with state of the art screen printing pastes.

For this reason, a large number of cell batches were processed in the last months, all based on large area industrial pre-processed Cz p-type material with an emitter sheet resistance of Rsh~90Ω/sq. Printed Al back surfaces as well as floating busbars (w_{BB} = 1.2mm)were applied previously to the dispensing step at Fraunhofer ISE's PVTEC. Single screen printed as well as double printed solar cells of the same material always served as reference groups with only the latter having floating busbars.

Applying a similar number of contact fingers (N=100), dispensed contact fingers allowed for a reduction of line width by a factor of 20% compared to both reference technologies in this batch. Consequently, a substantially improved j_{sc} in the range of +0.8 to 1.0 mA/cm² was reached with the dispensed group (Fig. 11, bottom, left).

Regarding the open circuit voltage, the floating busbar design allows for a slightly increased V_{oc} (Fig. 11, bottom, right) which is in good correlation to similar experiments [12]. A substantially decreased grid resistance at a slightly higher contact resistance leads to a FF level, that is in between both reference technologies and certainly allows for further improvements. Finally, cell efficiencies of up to 19.4% (Fig. 11, top, left) and thus an increase of 0.7% abs.

in comparison with previously published cell results on the same material [9] were reached thanks to a substantially improved dispensing paste and an advanced process stability. Both reference groups perform clearly less, mainly due to their known geometrical drawbacks, namely low aspect ratio and a substantially reduced finger homogeneity due to mesh marks (Fig. 7).

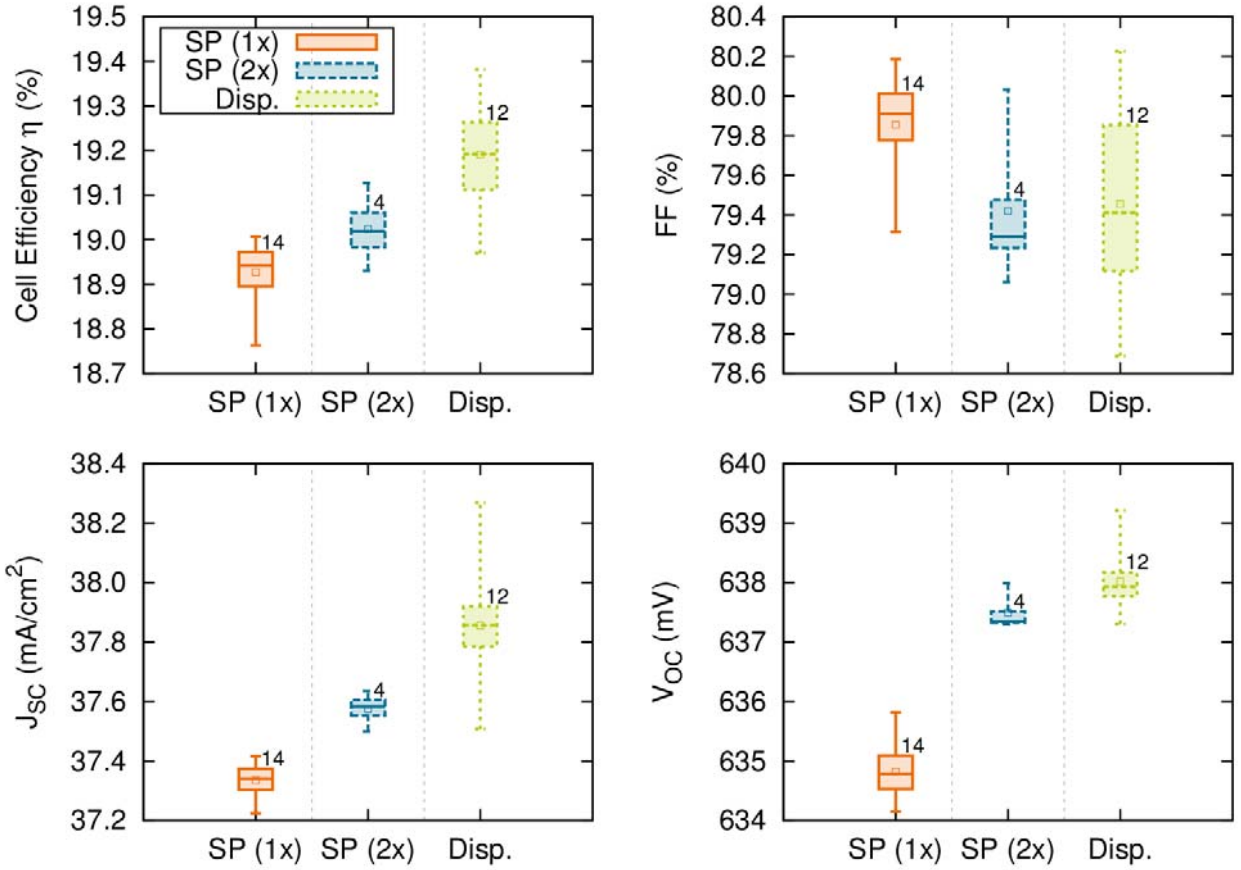

Fig. 11 IV-results of recent Al-BSF cell batch on industrial preprocessed Cz p-type material with an emitter sheet resistance of Rsh~90Ω/sq.

3.8. Solar cell results on PERC cell structures

In order to further demonstrate applicability of dispensing technology to advanced cell concepts, a batch on industrially preprocessed Cz p-type Si wafers with a passivated emitter and rear (PERC) cell structure and texture on both sides was conducted. Here, passivation on the back side was first opened locally by means of a screen printed etching paste prior to printing Ag-pads and Aluminum. On the front side, a floating busbar concept [12] was applied to all groups due to comparability reasons. Contact fingers of two reference groups were then applied via screen printing with an opening width of $w_s = 45\mu m$ giving a total of two (i.e. dual print) and three printing steps, respectively. A third group was then processed with dispensed contact fingers using a nozzle plate with opening width of $D = 60\mu m$. A variation of the peak firing temperature was further conducted with all groups. In Fig. 12, IV-results of the three cell groups at optimal firing temperature are shown, all measured in an industrial cell tester at PV-TEC.

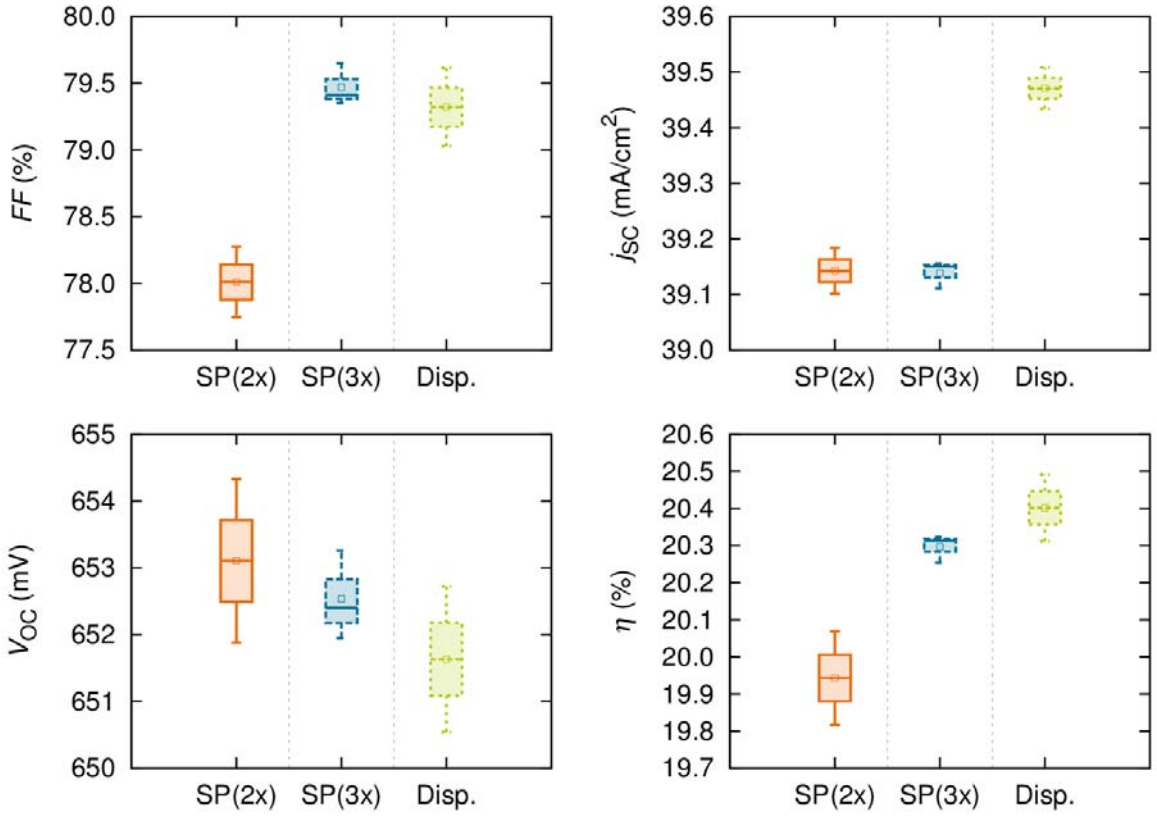

Fig. 12 IV-results of recent cell batch on industrial pre-processed and passivated Cz p-type material (PERC concept). All groups contain screen printed non-contacting busbars prior to the subsequent application of contact fingers by alternatively one or two additional screen printing steps or dispensing, respectively.

At similar contacting behaviour, the fill factor is strongly influenced by the resulting grid resistance. Consequently, the groups with double printed and dispensed contact fingers show substantially increased FF values than the samples with single screen printed contact fingers. As expected the j_{sc} values of dispensed contact fingers are increased due to substantially lower shading losses and an improved effective width. The V_{oc} is on a reasonably high level for all groups due to the applied PERC concept. The reason for slightly decreasing values in the double printed and the dispensed groups has not yet been completely identified but remains in the per mill range, comparatively. Finally, resulting cell efficiencies surpassed 20% for all groups, hence the concept of the locally opened passivation worked well for all samples. A maximum value of $\eta = 20.5\%$ was reached in the dispensed group giving an efficiency gain of $2\%_{rel.}$ ($0.4\%_{abs.}$) compared to the single screen printed group (here: dual printing) and $1\%_{rel.}$ ($0.2\%_{abs.}$) with respect to the group with double printed contact fingers.

4. Conclusions and outlook

Fast emerging thick film printing technologies remain a dynamic challenge for any kind of alternative metallization technology. The possibility to directly transfer results and findings from screen printing paste development however, allows for the enhancement of dispensing technology towards industrial cell processing.

Dispensed grid lines offer a substantially more homogeneous contact shape that require 20% less silver consumption as screen printed fingers to obtain similar grid resistances. Due to their high aspect ratio and a superior shape, an additional benefit results from a comparison of the two technologies regarding their effective finger width.

Here, an effective width of only 48% of their optical width contributes to shading in the encapsulate case which is substantially reduced to 73% obtained for screen printed contact fingers.

Consequently, increases in cell efficiencies of up to +0.4%abs. in comparison with standard single screen printing and +0.3%abs. with double printed reference were demonstrated on solar cells with industrial high-ohmic emitters. On industrially preprocessed PERC solar cells, a top value of $\eta = 20.5\%$ was reached with dispensing, giving an efficiency gain of $2\%_{rel.}$ ($0.4\%_{abs.}$) compared to a conventional dual screen printed reference group. With the new developed, inline applicable dispensing platform, a continuous printing process was demonstrated at printing speeds up to 700 mm·s-1. The integrated, advanced version of a ten nozzle parallel dispensing print head can be easily scaled for a future application in cell production.

Acknowledgements

The authors would like to thank all co-workers at the Photovoltaic Technology Evaluation Center (PV-TEC) and the mechanical workshop at Fraunhofer ISE for processing of the samples. This work was supported by the German Federal Ministry for Economic Affairs and Energy within the research project “GECKO” under contract number 0325404.

References

[1] H. Hannebauer *et al.*, Energy Procedia **43**, 66 (2013).
[2] B. Thaidigsmann *et al.*, Green **2**, 171 (2012).
[3] M. Beutel *et al.*, Solar Energy Materials and Solar Cells (2014).
[4] J. Specht *et al.*, in Proceedings of the 25th European Photovoltaic Solar Energy Conference and ExhibitionValencia, Spain, 2010), pp. 1867.
[5] E. Lohmüller *et al.*, IEEE Electron Device Letters **32**, 1719 (2011).
[6] M. Pospischil *et al.*, in 29th EU PVSEC (to be published, Amsterdam, 2014).
[7] M. Pospischil *et al.*, IEEE JPV **4**, 498 (2014).
[8] T. Fellmeth, F. Clement, and D. Biro, Photovoltaics, IEEE Journal of **4**, 504 (2014).
[9] M. Pospischil *et al.*, Energy Procedia **55**, 693 (2014).
[10] M. Pospischil *et al.*, Energy Procedia **43**, 111 (2013).
[11] M. Pospischil *et al.*, in Photovoltaic Specialists Conference (PVSC), 2013 IEEE 39th2013), pp. 2250.
[12] M. König *et al.*, Energy Procedia **27**, 1 (2012).
[13] R. Woehl, M. Hörteis, and S. W. Glunz Advances in OptoElectronics **2008** (2008).